Available online at www.sciencedirect.com
ScienceDirect
Signal Processing 88 (2008) 1327–1339
SIGNAL PROCESSING
www.elsevier.com/locate/sigpro

Extended 2q-MUSIC algorithm for noncircular signals

Jian Liu[a,*], Zhitao Huang[b], Yiyu Zhou[b]

[a]*Telecommunication Engineering College, Airforce Engineering University, Xi'an 710077, China*
[b]*School of Electronic Science and Engineering, National University of Defense Technology, Changsha 410073, China*

Received 28 October 2006; received in revised form 28 June 2007; accepted 16 November 2007
Available online 3 December 2007

Abstract

The NC-2q-MUSIC algorithm proposed in this paper is an extension of the 2q-MUSIC algorithm to the case of noncircular signals which are widely used in communication systems. The computational complexity of the NC-2q-MUSIC algorithm is analyzed in this paper and the NC-2q-MUSIC algorithm for uniform linear array (ULA), which, called NC-2q-MUSIC/ULA algorithm, needs much less computation, is also proposed. Due to the utilization of noncircular information of signals, the root mean square error (RMSE) performance of NC-2q-MUSIC algorithm is better than 2q-MUSIC algorithm for noncircular signals. And the NC-2q-MUSIC algorithm can handle more signals than 2q-MUSIC algorithm. It is proved that the robustness to modeling errors of NC-2q-MUSIC algorithm increases with q. Simulation results validate the better performance of NC-2q-MUSIC over 2q-MUSIC.

Keywords: Array signal processing; Direction finding; Aperture extension; Cumulants; MUSIC

1. Introduction

Since the beginning of the 1980s, many second-order high-resolution direction finding algorithms such as MUSIC [1] have been developed to overcome the limitations of the so-called super-resolution methods. Indeed, they are not able to process more than $M-1$ non-coherent signals from an array of M sensors, are sensitive to the modeling errors and are difficult to resolve several poorly angularly spaced signals from a limited number of snapshots. The MUSIC-like algorithm [2] based on fourth-order cumulants introduced in the beginning of 1990s extends the array aperture and overcomes the previous limitations to some extent [3]. Recently, Chevalier et al. [4] developed an extension of MUSIC algorithm to arbitrary even-order 2q ($q \geqslant 1$), giving rise to the so-called 2q-MUSIC algorithms, which can handle more signals, can resolve more poorly angularly separated signals and are more robust with the increase of q.

In recent years, direction finding for noncircular signals, e.g., binary phased-shift keying (BPSK) modulated signals which are widely used in communication systems, has attracted more and more attention due to the performance gain from the noncircular properties. In 1998, Galy proposed a MUSIC-like algorithm for noncircular signals (called NC-MUSIC algorithm), and subsequently Charge et al. [5] proposed the root-MUSIC-like algorithm for noncircular signals in 2001, and Haardt and Romer [6] proposed the unitary ESPRIT-like algorithm for noncircular signals in

*Corresponding author.
E-mail address: sdwfliuj@163.com (J. Liu).

0165-1684/$ - see front matter © 2007 Elsevier B.V. All rights reserved.
doi:10.1016/j.sigpro.2007.11.012

2004. Observed by simulations, the above algorithms can handle more sources than the number of sensors and can significantly improve the accuracy of direction-of-arrival (DOA) estimate. Delmas and Abeida proved the performance bound of algorithms for noncircular signals [7–9].

Similar to NC-MUSIC algorithm, an extension of 2-MUSIC, the NC-2q-MUSIC algorithm proposed in this paper extends the 2q-MUSIC algorithm to noncircular applications. The NC-2q-MUSIC algorithm has better estimation accuracy, larger estimation capacity and is more robust to modeling errors than the 2q-MUSIC algorithm of the same order. The NC-2q-MUSIC algorithms are more robust to modeling errors with the increase of q.

The paper is organized as follows. In Section 2, the signal model and the concept of noncircularity are introduced. In Section 3, we recall the 2q-MUSIC algorithm which is the foundation of our proposed NC-2q-MUSIC algorithm. The NC-2q-MUSIC algorithm and its simplified version for ULA, together with the analysis of their computational complexities are presented in Section 4. It is proved in Section 5 that the robustness of the NC-2q-MUSIC algorithm increases with q, and the NC-2q-MUSIC algorithm is always more robust than the 2q-MUSIC algorithm with the same order. The better performance of the NC-2q-MUSIC algorithm compared with the 2q-MUSIC algorithm is validated by the simulations in Section 6. Finally, Section 7 concludes this paper.

2. Problem formulation

2.1. Signal modeling

We consider D statistically independent narrowband plane wave signals impinging on an array of M identical omnidirectional sensors. Our discussion is confined to azimuth-only systems, i.e., the sensors and signals are assumed to be co-planar. The signal number D is assumed to be known or be obtained by estimation. The superscript "*", "T" and "H" denote the conjugate, the transpose and the conjugate transpose, respectively. The outputs of the M array elements at time t are arranged in an $M \times 1$ vector

$$\boldsymbol{x}(t) = [x_1(t), x_2(t), \ldots, x_M(t)]^{\mathrm{T}} = \boldsymbol{A}\boldsymbol{s}(t) + \boldsymbol{n}(t), \qquad (1)$$

where $\boldsymbol{s}(t) = [s_1(t),\ s_2(t),\ \ldots,\ s_D(t)]^{\mathrm{T}}$ is the signal vector, $\boldsymbol{n}(t) = [n_1(t),\ n_2(t),\ \ldots,\ n_M(t)]^{\mathrm{T}}$ is the noise vector, $\boldsymbol{A} = [\boldsymbol{a}(\theta_1),\ \boldsymbol{a}(\theta_2),\ \ldots,\ \boldsymbol{a}(\theta_D)]$ is the steering matrix

$$\boldsymbol{a}(\theta) = \left[\mathrm{e}^{-\mathrm{j}2\pi/\lambda(d_{x,1}\cos\theta + d_{y,1}\sin\theta)}, \ldots, \mathrm{e}^{-\mathrm{j}2\pi/\lambda(d_{x,M}\cos\theta + d_{y,M}\sin\theta)}\right]^{\mathrm{T}}$$

is the steering vector, λ is the wavelength of the carrier, and $(d_{x,i}, d_{y,i})$ are the coordinates of sensor i (assuming the first sensor locates at the origin, i.e., $d_{x,1} = 0$, $d_{y,1} = 0$). We assume that $s_i(t)$ ($i = 1, 2, \ldots, D$) is zero-mean stationary random process with the variance $\sigma_{s,i}^2$, that $n_i(t)$ is a complex circular Gaussian white noise with the variance σ_n^2, and that the signals and noises are statistically independent. We also assume that the signals are non-Gaussian because the higher-order cumulant of Gaussian signal is zero and the 2qth-order ($q \geqslant 2$) cumulants will be used in the proposed algorithm. For notational convenience, the time index t will be omitted when there is no possibility of confusion.

2.2. Circularity and noncircularity

Here we only use the first- and second-order statistical properties of the signals. Definition of circularity of order 2 is very simple. For a complex random signal s, the only moments to be considered are the mean $E\{s\}$, the covariance $E\{ss^*\}$, and the elliptic covariance $E\{ss\}$. A complex random variable is said to be circular of the order 2 if its first and second statistical properties are rotational invariant for an arbitrary phase φ, i.e.

$$E\{s\mathrm{e}^{\mathrm{j}\varphi}\} = E\{s\}, \qquad (2)$$

$$E\{s\mathrm{e}^{\mathrm{j}\varphi}(s\mathrm{e}^{\mathrm{j}\varphi})^*\} = E\{ss^*\}, \qquad (3)$$

$$E\{s\mathrm{e}^{\mathrm{j}\varphi} \cdot s\mathrm{e}^{\mathrm{j}\varphi}\} = E\{ss\}. \qquad (4)$$

Since the signals are assumed to be zero-mean in this paper, i.e. $E\{s\} = 0$, (2) is obvious, (3) is satisfied naturally and (4) is satisfied if $E\{ss\} = 0$. The signals are non-zero, so we have $E\{ss^*\} = 0$. Then the fact that s is circular is equivalent to $E\{s\} = 0$, $E\{ss^*\} \neq 0$ and $E\{ss\} = 0$. The signal s is said to be noncircular, if the first- and second-order statistical properties of the signal are not rotational invariant, i.e. $E\{ss\} \neq 0$. The classical high-resolution direction finding algorithms are designed for circular signals, without employing the information in $E\{ss\}$. The direction finding algorithms for noncircular signals employ the information in $E\{ss^*\}$ as

well as in $E\{ss\}$. These algorithms have improved performance since more information is employed.

For an arbitrary signal s, we obtain [7]

$$E\{s^2\} = \rho e^{j\phi} E\{ss^*\} = \rho e^{j\phi}\sigma_s^2, \tag{5}$$

where ϕ is the noncircularity phase and ρ is the noncircularity rate which satisfies $0 \leqslant \rho \leqslant 1$ (from Cauchy–Schwartz inequality). Obviously, the signals which satisfy $0 < \rho \leqslant 1$ are noncircular. The noncircularity rate ρ is determined by the modulation of the signal, e.g., $\rho = 1$ for unfiltered BPSK signals. Let $s_0 = s e^{-j\phi/2}$ and $\rho = 1$, it can be obtained from (5) that

$$E\{s_0^2\} = E\{s_0 s_0^*\}. \tag{6}$$

Obviously, s_0 can be written as

$$s_0 = s_R + j s_I, \tag{7}$$

where s_R and s_I are the real and imaginary parts of s_0, respectively. By introducing (7) into (6), we can yield

$$E\{s_R^2\} - E\{s_I^2\} - j2E\{s_R s_I\} = E\{s_R^2\} + E\{s_I^2\}. \tag{8}$$

If (8) is satisfied, there must be $s_I = 0$. Therefore, for the case of $\rho = 1$, the noncircular signals impinging on the array can be expressed as [6]

$$\boldsymbol{s} = \boldsymbol{\Phi}^{1/2}\boldsymbol{s}_0, \tag{9}$$

where $\boldsymbol{s}_0 = [s_{0,1}, s_{0,2}, \ldots, s_{0,D}]^T \in \mathbb{R}$, $s_{0,i}$ is the zero-phase version of the signal s_i and the diagonal matrix $\boldsymbol{\Phi}^{1/2} = \mathrm{diag}\{e^{j\phi_i/2}\}_{i=1}^{D}$ contains arbitrary phase shifts which are the phases of the signals.

3. 2q-MUSIC algorithm

3.1. 2qth-order cumulant matrix

The classical direction finding algorithms are based on the second-order statistics (the covariance matrix is indeed the second-order cumulant matrix). Higher-order cumulants have the ability to reconstruct the phase of nonminimum phase systems and are insensitive to Gaussian noise. Due to these properties, higher-order cumulant is widely used in signal processing. The odd-order cumulant is zero for the symmetrically distributed random variables and is very small for the nonsymmetrically distributed random variables while the even-order cumulant in these cases is relatively large. Hence, it is preferred to the even-order cumulant rather than the odd-order cumulant. For zero-mean complex random variables $x_{k_1}, x_{k_2}, \ldots, x_{k_{2q}} (k_1, k_2, \ldots, k_{2q} \in \{1, 2, \ldots, M\}, \quad q = 1, 2, \ldots)$, the $2q$th-order cumulant is denoted as $\mathrm{cum}(x_{k_1}, x_{k_2}, \ldots, x_{k_{2q}})$. Explicit expressions of $\mathrm{cum}(x_{k_1}, x_{k_2}, \ldots, x_{k_{2q}})$ for $1 \leqslant q \leqslant 3$ are given in [10]. Consider the indices defined by

$$I_{k_1,\ldots,k_q} = \sum_{i=1}^{q} M^{q-i}(k_i - 1) + 1, \tag{10}$$

$$J_{k_{q+1},\ldots,k_{2q}} = \sum_{i=1}^{q} M^{q-i}(k_{q+i} - 1) + 1. \tag{11}$$

Let

$$\gamma_i = \mathrm{cum}(\underbrace{s_{0,i}, s_{0,i}, \ldots, s_{0,i}}_{2q})$$

and

$$\boldsymbol{\Gamma} = \mathrm{diag}\{\gamma_1, \gamma_2, \ldots, \gamma_D\},$$

from (9) we obtain

$$\mathrm{cum}(\underbrace{s_i, s_i, \ldots, s_i}_{2q}) = \gamma_i e^{jq\phi_i}.$$

Let $\mathrm{cum}(x_{k_1}, x_{k_2}, \ldots, x_{k_{2q}})$ be the $I_{k_1,\ldots,k_q}$th row and the $J_{k_{q+1},\ldots,k_{2q}}$th column of $M^q \times M^q$ matrix $\boldsymbol{Q}_x$. According to the properties of higher-order cumulants CP4, CP3 and CP1 in [3], we get $\boldsymbol{Q}_x = \boldsymbol{B}\boldsymbol{\Gamma}\boldsymbol{\Phi}^q\boldsymbol{B}^T$, where $\boldsymbol{B} = [\boldsymbol{b}(\theta_1), \boldsymbol{b}(\theta_2), \ldots, \boldsymbol{b}(\theta_D)]$, $\boldsymbol{b}(\theta) = \boldsymbol{a}(\theta)^{\otimes q}$, "$\otimes$" is the Kronecker product, and $\boldsymbol{a}(\theta)^{\otimes q}$ is defined by $\boldsymbol{a}(\theta)^{\otimes q} = \boldsymbol{a}(\theta) \otimes \boldsymbol{a}(\theta) \otimes \cdots \otimes \boldsymbol{a}(\theta)$ with a number of Kronecker product "$\otimes$" equal to $q-1$, with the convention $\boldsymbol{a}(\theta)^{\otimes 0} = 1$.

For convenience, we define the operator CUM as follows: the arrangement of the elements of $\mathrm{CUM}([\boldsymbol{x}^{\otimes q}][\boldsymbol{x}^{\otimes q}]^T)$ is the same as that of $\mathrm{cum}(x_{k_1}, x_{k_2}, \ldots, x_{k_{2q}})$, i.e., similar to the fact that the $I_{k_1,\ldots,k_q}$th row and the $J_{k_{q+1},\ldots,k_{2q}}$th column element of $[\boldsymbol{x}^{\otimes q}][\boldsymbol{x}^{\otimes q}]^T$ is $x_{k_1}, x_{k_2}, \ldots, x_{k_{2q}}$, the $I_{k_1,\ldots,k_q}$th row and the $J_{k_{q+1},\ldots,k_{2q}}$th column element of $\mathrm{CUM}([\boldsymbol{x}^{\otimes q}][\boldsymbol{x}^{\otimes q}]^T)$ is $\mathrm{cum}(x_{k_1}, x_{k_2}, \ldots, x_{k_{2q}})$. Then, the cumulant matrix $\boldsymbol{Q}_x$ can be expressed as $\mathrm{CUM}([\boldsymbol{x}^{\otimes q}][\boldsymbol{x}^{\otimes q}]^T)$.

3.2. 2q-MUSIC algorithm [4]

Let

$$\boldsymbol{Q}_{x1} = \mathrm{CUM}([\boldsymbol{x}^{\otimes l} \otimes \boldsymbol{x}^{*\otimes(q-l)}][\boldsymbol{x}^{\otimes l} \otimes \boldsymbol{x}^{*\otimes(q-l)}]^H),$$

$$\boldsymbol{b}_1(\theta) = \boldsymbol{a}(\theta)^{\otimes l} \otimes \boldsymbol{a}(\theta)^{*\otimes(q-l)},$$

and

$$\boldsymbol{B}_1 = [\boldsymbol{b}_1(\theta_1), \boldsymbol{b}_1(\theta_2), \ldots, \boldsymbol{b}_1(\theta_D)],$$

where l is an integer with $0 \leqslant l \leqslant q$, for $q > 1$, we get

$$\boldsymbol{Q}_{x1} = \boldsymbol{B}_1\boldsymbol{\Gamma}\boldsymbol{B}_1^H. \tag{12}$$

To use the matrix $\boldsymbol{Q}_{x1}$ in the $2q$-MUSIC algorithm, we first compute the singular value decomposition (SVD):

$$\boldsymbol{Q}_{x1} = \begin{bmatrix} \boldsymbol{U}_1 & \boldsymbol{U}_2 \end{bmatrix} \begin{bmatrix} \boldsymbol{\Sigma}_1 & \boldsymbol{O} \\ \boldsymbol{O} & \boldsymbol{O} \end{bmatrix} \begin{bmatrix} \boldsymbol{V}_1^{\mathrm{H}} \\ \boldsymbol{V}_2^{\mathrm{H}} \end{bmatrix}, \tag{13}$$

where the columns of $\boldsymbol{U}_1$ span the signal subspace and the columns of $\boldsymbol{U}_2$ span the noise subspace, and $\boldsymbol{\Sigma}_1$ is a $D \times D$ diagonal matrix. Here, the steering vector extends to $\boldsymbol{a}(\theta)^{\otimes l} \otimes \boldsymbol{a}(\theta)^{*\otimes(q-l)}$. As in the case of the standard MUSIC algorithm, when θ is the real DOA of the signal, the steering vector $\boldsymbol{b}_1(\theta)$ is orthogonal to the columns of $\boldsymbol{U}_2$. We use this fact to form the null-spectrum of $2q$-MUSIC algorithm

$$f_{2q-\mathrm{MUSIC}}(\theta) = \boldsymbol{b}_1^{\mathrm{H}}(\theta)\boldsymbol{U}_2\boldsymbol{U}_2^{\mathrm{H}}\boldsymbol{b}_1(\theta). \tag{14}$$

4. $2q$-MUSIC algorithm for noncircular signals: NC-$2q$-MUSIC algorithm

4.1. NC-2q-MUSIC algorithm

For $q = 1$, the NC-MUSIC (i.e., NC-2-MUSIC) algorithm extends the 2-MUSIC algorithm to noncircular applications. In this subsection, we extend this result to $2q$th-order. For $q > 1$, let $\boldsymbol{b}_2(\theta) = \boldsymbol{a}(\theta)^{\otimes q}$, $\boldsymbol{B}_2 = [\boldsymbol{b}_2(\theta_1), \boldsymbol{b}_2(\theta_2), \ldots, \boldsymbol{b}_2(\theta_D)]$, we can easily obtain

$$\begin{aligned} \boldsymbol{Q}_{x1} &= \mathrm{CUM}([\boldsymbol{x}^{\otimes l} \otimes \boldsymbol{x}^{*\otimes(q-l)}][\boldsymbol{x}^{\otimes l} \otimes \boldsymbol{x}^{*\otimes(q-l)}]^{\mathrm{H}}) \\ &= \sum_{i=1}^{D} \boldsymbol{b}_1(\theta_i)\boldsymbol{b}_1^{\mathrm{H}}(\theta_i)\gamma_i = \boldsymbol{B}_1\boldsymbol{\Gamma}\boldsymbol{B}_1^{\mathrm{H}}, \end{aligned} \tag{15}$$

$$\begin{aligned} \boldsymbol{Q}_{x2} &= \mathrm{CUM}([\boldsymbol{x}^{\otimes l} \otimes \boldsymbol{x}^{*\otimes(q-l)}][\boldsymbol{x}^{\otimes q}]^{\mathrm{T}}) \\ &= \sum_{i=1}^{D} \boldsymbol{b}_1(\theta_i)\boldsymbol{b}_2^{\mathrm{T}}(\theta_i)\gamma_i\, \mathrm{e}^{\mathrm{j}l\phi_i} = \boldsymbol{B}_1\boldsymbol{\Gamma}\boldsymbol{\Phi}^{l}\boldsymbol{B}_2^{\mathrm{T}}, \end{aligned} \tag{16}$$

$$\begin{aligned} \boldsymbol{Q}_{x3} &= \mathrm{CUM}([\boldsymbol{x}^{\otimes q}]^{*}[\boldsymbol{x}^{\otimes q}]^{\mathrm{T}}) \\ &= \sum_{i=1}^{D} \boldsymbol{b}_2^{*}(\theta_i)\boldsymbol{b}_2^{\mathrm{T}}(\theta_i)\gamma_i = \boldsymbol{B}_2^{*}\boldsymbol{\Gamma}\boldsymbol{B}_2^{\mathrm{T}}. \end{aligned} \tag{17}$$

Obviously, the noncircular information $\boldsymbol{\Phi}$ is embedded in matrix $\boldsymbol{Q}_{x2}$, while none in matrix $\boldsymbol{Q}_{x1}$ and $\boldsymbol{Q}_{x3}$. The performance of $2q$-MUSIC algorithm is not so good because only $\boldsymbol{Q}_{x1}$ is functional. The NC-$2q$-MUSIC algorithm proposed in this paper employs $\boldsymbol{Q}_{x1}$, $\boldsymbol{Q}_{x2}$ and $\boldsymbol{Q}_{x3}$ altogether to improve the performance. We get the extended $2M^q \times 2M^q$ $2q$th-order cumulant matrix $\boldsymbol{Q}_{\mathrm{E}}$ by the three $M^q \times M^q$ $2q$th-order cumulant matrices defined by (15)–(17):

$$\begin{aligned} \boldsymbol{Q}_{\mathrm{E}} &= \begin{bmatrix} \boldsymbol{Q}_{x1} & \boldsymbol{Q}_{x2} \\ \boldsymbol{Q}_{x2}^{\mathrm{H}} & \boldsymbol{Q}_{x3} \end{bmatrix} = \begin{bmatrix} \boldsymbol{B}_1\boldsymbol{\Gamma}\boldsymbol{B}_1^{\mathrm{H}} & \boldsymbol{B}_1\boldsymbol{\Gamma}\boldsymbol{\Phi}^{l}\boldsymbol{B}_2^{\mathrm{T}} \\ \boldsymbol{B}_2^{*}\boldsymbol{\Phi}^{-l}\boldsymbol{\Gamma}\boldsymbol{B}_1^{\mathrm{H}} & \boldsymbol{B}_2^{*}\boldsymbol{\Gamma}\boldsymbol{B}_2^{\mathrm{T}} \end{bmatrix} \\ &= \begin{bmatrix} \boldsymbol{B}_1 \\ \boldsymbol{B}_2^{*}\boldsymbol{\Phi}^{-l} \end{bmatrix} \boldsymbol{\Gamma} \begin{bmatrix} \boldsymbol{B}_1 \\ \boldsymbol{B}_2^{*}\boldsymbol{\Phi}^{-l} \end{bmatrix}^{\mathrm{H}}. \end{aligned} \tag{18}$$

The matrix $\boldsymbol{Q}_{\mathrm{E}}$ contains noncircular information because $\boldsymbol{Q}_{x2}$ appears in it. Thereby the steering matrix extends to

$$\begin{bmatrix} \boldsymbol{B}_1 \\ \boldsymbol{B}_2^{*}\boldsymbol{\Phi}^{-l} \end{bmatrix}$$

and the corresponding aperture of the array is extended. The SVD of $\boldsymbol{Q}_{\mathrm{E}}$ is given by

$$\boldsymbol{Q}_{\mathrm{E}} = \begin{bmatrix} \boldsymbol{U}_s & \boldsymbol{U}_n \end{bmatrix} \begin{bmatrix} \boldsymbol{\Sigma}_{\mathrm{s}} & \boldsymbol{O} \\ \boldsymbol{O} & \boldsymbol{O} \end{bmatrix} \begin{bmatrix} \boldsymbol{V}_s^{\mathrm{H}} \\ \boldsymbol{V}_n^{\mathrm{H}} \end{bmatrix}, \tag{19}$$

where $\boldsymbol{\Sigma}_{\mathrm{s}}$ is the diagonal matrix of singular values which are arranged in the decreasing order, and the columns of $\boldsymbol{U}_n$ span the noise subspace. The DOAs of the signals are given by the minima of the following spatial spectrum function:

$$f(\theta, \phi) = \boldsymbol{b}^{\mathrm{H}}(\theta, \phi)\boldsymbol{U}_n\boldsymbol{U}_n^{\mathrm{H}}\boldsymbol{b}(\theta, \phi), \tag{20}$$

where

$$\boldsymbol{b}(\theta, \phi) = \begin{bmatrix} \boldsymbol{b}_1(\theta) \\ \boldsymbol{b}_2^{*}(\theta)\, \mathrm{e}^{-\mathrm{j}l\phi} \end{bmatrix}$$

is the extended steering vector. Therefore, we have to search for local minima over θ and ϕ. To alleviate the computational complexity, the 2-D search is substituted with 1-D search by the following method. We partition $\boldsymbol{U}_n$ into the two submatrices with the same dimension [5]

$$\boldsymbol{U}_n = \begin{bmatrix} \boldsymbol{U}_{n1} \\ \boldsymbol{U}_{n2} \end{bmatrix}. \tag{21}$$

Replacing (21) into (20) yields

$$\begin{aligned} & f(\theta, \phi) \\ &= \boldsymbol{b}^{\mathrm{H}}(\theta, \phi) \begin{bmatrix} \boldsymbol{U}_{n1}\boldsymbol{U}_{n1}^{\mathrm{H}} & \boldsymbol{U}_{n1}\boldsymbol{U}_{n2}^{\mathrm{H}} \\ \boldsymbol{U}_{n2}\boldsymbol{U}_{n1}^{\mathrm{H}} & \boldsymbol{U}_{n2}\boldsymbol{U}_{n2}^{\mathrm{H}} \end{bmatrix} \boldsymbol{b}(\theta, \phi) \\ &= \boldsymbol{q}^{\mathrm{H}} \begin{bmatrix} \boldsymbol{b}_1^{\mathrm{H}}(\theta)\boldsymbol{U}_{n1}\boldsymbol{U}_{n1}^{\mathrm{H}}\mathbf{b}_1(\theta) & \boldsymbol{b}_1^{\mathrm{H}}(\theta)\boldsymbol{U}_{n1}\boldsymbol{U}_{n2}^{\mathrm{H}}\boldsymbol{b}_2^{*}(\theta) \\ (\boldsymbol{b}_1^{\mathrm{H}}(\theta)\boldsymbol{U}_{n1}\boldsymbol{U}_{n2}^{\mathrm{H}}\mathbf{b}_2^{*}(\theta))^{\mathrm{H}} & \boldsymbol{b}_2^{\mathrm{T}}(\theta)\boldsymbol{U}_{n2}\boldsymbol{U}_{n2}^{\mathrm{H}}\boldsymbol{b}_2^{*}(\theta) \end{bmatrix} \boldsymbol{q} \end{aligned} \tag{22}$$

with

$$\boldsymbol{q}=\begin{bmatrix}1\\ \mathrm{e}^{-\mathrm{j}l\phi}\end{bmatrix}.$$

Let the partial difference of (22) equal to zero, i.e., $\partial f(\theta,\phi)/\partial\phi=0$, we obtain

$$\mathrm{e}^{\mathrm{j}l\phi}=\pm\frac{\boldsymbol{b}_1^{\mathrm{H}}(\theta)\boldsymbol{U}_{n1}\boldsymbol{U}_{n2}^{\mathrm{H}}\boldsymbol{b}_2^{*}(\theta)}{\left\|\boldsymbol{b}_1^{\mathrm{H}}(\theta)\boldsymbol{U}_{n1}\boldsymbol{U}_{n2}^{\mathrm{H}}\boldsymbol{b}_2^{*}(\theta)\right\|}. \tag{23}$$

The minima of (20) are obtained when the sign of the right-hand side of (23) is minus. Therefore the spatial spectrum function of NC-2q-MUSIC algorithm is given by

$$f(\theta)=\boldsymbol{b}_1^{\mathrm{H}}(\theta)\boldsymbol{U}_{n1}\boldsymbol{U}_{n1}^{\mathrm{H}}\boldsymbol{b}_1(\theta)+\boldsymbol{b}_2^{\mathrm{T}}(\theta)\boldsymbol{U}_{n2}\boldsymbol{U}_{n2}^{\mathrm{H}}\boldsymbol{b}_2^{*}(\theta)-2\left\|\boldsymbol{b}_1^{\mathrm{H}}(\theta)\boldsymbol{U}_{n1}\boldsymbol{U}_{n2}^{\mathrm{H}}\boldsymbol{b}_2^{*}(\theta)\right\|. \tag{24}$$

Conclusively, the processes of NC-2q-MUSIC algorithm are as follows:

Step 1: Compute the three $M^q\times M^q$ 2qth-order cumulant matrices $\boldsymbol{Q}_{x1}$, $\boldsymbol{Q}_{x2}$ and $\boldsymbol{Q}_{x3}$.

Step 2: Obtain the $2M^q\times 2M^q$ 2qth-order cumulant matrix $\boldsymbol{Q}_{\mathrm{E}}$ using (18).

Step 3: Compute the SVD of matrix $\boldsymbol{Q}_{\mathrm{E}}$ to obtain $\boldsymbol{U}_n$.

Step 4: Search for the minima of spatial spectrum function (24) to get the DOAs of the signals.

In order to achieve the accurate DOA estimation in practice, a large number of snapshots are needed to precisely estimate the cumulants. It can be satisfied in some practical applications such as in tracking radars and communication systems. Then the computational burden is an important problem, which will be discussed in the following subsection.

4.2. Computational complexity of NC-2q-MUSIC algorithm

In situations of practical interest, the 2qth-order cumulants are not known *a priori* and have to be estimated from samples of data. Taking $q=2$ for example, the estimate of fourth-order cumulant $\mathrm{cum}(x_{k_1},x_{k_2},x_{k_3},x_{k_4})$ can be expressed as [11]

$$\begin{aligned}\hat{c}(k_1,k_2,k_3,k_4)&=\frac{1}{\alpha}\sum_{t=1}^{L}x_{k_1}(t)x_{k_2}(t)x_{k_3}(t)x_{k_4}(t)\\&\quad-\frac{1}{\beta}\sum_{t=1}^{L}x_{k_1}(t)x_{k_2}(t)\sum_{t=1}^{L}x_{k_3}(t)x_{k_4}(t)\\&\quad-\frac{1}{\beta}\sum_{t=1}^{L}x_{k_1}(t)x_{k_3}(t)\sum_{t=1}^{L}x_{k_2}(t)x_{k_4}(t)\\&\quad-\frac{1}{\beta}\sum_{t=1}^{L}x_{k_1}(t)x_{k_4}(t)\sum_{t=1}^{L}x_{k_2}(t)x_{k_3}(t),\end{aligned} \tag{25}$$

where α and β are functions of L which denotes the number of snapshots. Eq. (25) is an unbiased estimator of fourth-order cumulant when $L>1$, $\alpha=(L^2-L)/(L+2)$, $\beta=L^2-L$ and a biased estimator when $L>0$, $\alpha=L$, $\beta=L^2$. Every element of the fourth-order cumulant matrices $\boldsymbol{Q}_{x1}$, $\boldsymbol{Q}_{x2}$ and $\boldsymbol{Q}_{x3}$ can be obtained from (25).

For zero-mean random variables, the complexity to compute a fourth-order cumulant is about $9L$ multiplications according to (25). Since all the three matrices $\boldsymbol{Q}_{x1}$, $\boldsymbol{Q}_{x2}$ and $\boldsymbol{Q}_{x3}$ are $M^2\times M^2$, the complexity to compute $\boldsymbol{Q}_{\mathrm{E}}$ is about $27M^4L$ multiplications and the computation of the SVD of $2M^2\times 2M^2$ matrix $\boldsymbol{Q}_{\mathrm{E}}$ is about $\mathrm{O}(8M^6)$ (i.e. the order of $8M^6$) multiplications. Therefore, the total computation of NC-4-MUSIC algorithm is about $27M^4L+\mathrm{O}(8M^6)$ multiplications. Similarly, for $q=3$, the total computation of NC-6-MUSIC algorithm is about $450M^6L+\mathrm{O}(8M^9)$ multiplications.

It is easy to see that the computation of NC-2q-MUSIC algorithm increases rapidly as the number of sensors increases. Fortunately, for uniform linear array (ULA), the computation can be significantly reduced by taking off the redundant elements from $\boldsymbol{Q}_{\mathrm{E}}$, as is shown below.

4.3. NC-2q-MUSIC/ULA algorithm

For the NC-2q-MUSIC algorithm with ULA and $q\geqslant 2$, there are many redundant elements in $\boldsymbol{Q}_{\mathrm{E}}$. These elements carry no information about DOA while aggravating the computation. For ULA, there is a method to remove the redundant elements. We call the NC-2q-MUSIC algorithm using this method the NC-2q-MUSIC/ULA algorithm.

Before introducing the NC-2q-MUSIC/ULA algorithm, we define

$$\bar{\boldsymbol{x}}=\begin{bmatrix}x_1\\ x_M\end{bmatrix},\quad \bar{\boldsymbol{a}}(\theta)=\begin{bmatrix}a_1(\theta)\\ a_M(\theta)\end{bmatrix},$$

$$\bar{\boldsymbol{A}}=[\bar{\boldsymbol{a}}(\theta_1),\bar{\boldsymbol{a}}(\theta_2),\ldots,\bar{\boldsymbol{a}}(\theta_D)],$$

$$\bar{\boldsymbol{b}}_1(\theta)=\bar{\boldsymbol{a}}(\theta)^{\otimes l}\otimes\bar{\boldsymbol{a}}(\theta)^{*\otimes(q-l-1)}\otimes\boldsymbol{a}(\theta)^{*},$$

$$\bar{\boldsymbol{b}}_2(\theta)=\bar{\boldsymbol{a}}(\theta)^{\otimes(q-1)}\otimes\boldsymbol{a}(\theta),$$

$$\bar{\boldsymbol{B}}_1=[\bar{\boldsymbol{b}}_1(\theta_1),\bar{\boldsymbol{b}}_1(\theta_2),\ldots,\bar{\boldsymbol{b}}_1(\theta_D)]$$

and

$$\bar{\boldsymbol{B}}_2 = [\bar{\boldsymbol{b}}_2(\theta_1), \bar{\boldsymbol{b}}_2(\theta_2), \ldots, \bar{\boldsymbol{b}}_2(\theta_D)].$$

Similar to (15)–(17), with $q \geqslant 2$, we obtain

$$\begin{aligned}\bar{\boldsymbol{Q}}_{x1} &= \mathrm{CUM}([\bar{\boldsymbol{x}}^{\otimes l} \otimes \bar{\boldsymbol{x}}^{*\otimes(q-l-1)} \otimes \boldsymbol{x}^*] \\ &\quad \times [\bar{\boldsymbol{x}}^{\otimes l} \otimes \bar{\boldsymbol{x}}^{*\otimes(q-l-1)} \otimes \boldsymbol{x}^*]^{\mathrm{H}}) \\ &= \sum_{i=1}^{D} \bar{\boldsymbol{b}}_1(\theta_i)\bar{\boldsymbol{b}}_1^{\mathrm{H}}(\theta_i)\gamma_i = \bar{\boldsymbol{B}}_1 \boldsymbol{\Gamma} \bar{\boldsymbol{B}}_1^{\mathrm{H}}, \end{aligned} \tag{26}$$

$$\begin{aligned}\bar{\boldsymbol{Q}}_{x2} &= \mathrm{CUM}([\bar{\boldsymbol{x}}^{\otimes l} \otimes \bar{\boldsymbol{x}}^{*\otimes(q-l-1)} \otimes \boldsymbol{x}^*][\bar{\boldsymbol{x}}^{\otimes(q-1)} \otimes \boldsymbol{x}]^{\mathrm{T}}) \\ &= \sum_{i=1}^{D} \bar{\boldsymbol{b}}_1(\theta_i)\bar{\boldsymbol{b}}_2^{\mathrm{T}}(\theta_i)\gamma_i \, \mathrm{e}^{\mathrm{j}l\phi_i} = \bar{\boldsymbol{B}}_1 \boldsymbol{\Gamma} \boldsymbol{\Phi}^l \bar{\boldsymbol{B}}_2^{\mathrm{T}}, \end{aligned} \tag{27}$$

$$\begin{aligned}\bar{\boldsymbol{Q}}_{x3} &= \mathrm{CUM}([\bar{\boldsymbol{x}}^{\otimes(q-1)} \otimes \boldsymbol{x}]^*[\bar{\boldsymbol{x}}^{\otimes(q-1)} \otimes \boldsymbol{x}]^{\mathrm{T}}) \\ &= \sum_{i=1}^{D} \bar{\boldsymbol{b}}_2^*(\theta_i)\bar{\boldsymbol{b}}_2^{\mathrm{T}}(\theta_i)\gamma_i = \bar{\boldsymbol{B}}_2^* \boldsymbol{\Gamma} \bar{\boldsymbol{B}}_2^{\mathrm{T}}. \end{aligned} \tag{28}$$

Similar to (18), the extended $2q$th-order cumulant matrix is given by

$$\begin{aligned}\bar{\boldsymbol{Q}}_{\mathrm{E}} &= \begin{bmatrix} \bar{\boldsymbol{Q}}_{x1} & \bar{\boldsymbol{Q}}_{x2} \\ \bar{\boldsymbol{Q}}_{x2}^{\mathrm{H}} & \bar{\boldsymbol{Q}}_{x3} \end{bmatrix} = \begin{bmatrix} \bar{\boldsymbol{B}}_1 \boldsymbol{\Gamma} \bar{\boldsymbol{B}}_1^{\mathrm{H}} & \bar{\boldsymbol{B}}_1 \boldsymbol{\Gamma} \boldsymbol{\Phi}^l \bar{\boldsymbol{B}}_2^{\mathrm{T}} \\ \bar{\boldsymbol{B}}_2^* \boldsymbol{\Phi}^{-l} \boldsymbol{\Gamma} \bar{\boldsymbol{B}}_1^{\mathrm{H}} & \bar{\boldsymbol{B}}_2^* \boldsymbol{\Gamma} \bar{\boldsymbol{B}}_2^{\mathrm{T}} \end{bmatrix} \\ &= \begin{bmatrix} \bar{\boldsymbol{B}}_1 \\ \bar{\boldsymbol{B}}_2^* \boldsymbol{\Phi}^{-l} \end{bmatrix} \boldsymbol{\Gamma} \begin{bmatrix} \bar{\boldsymbol{B}}_1 \\ \bar{\boldsymbol{B}}_2^* \boldsymbol{\Phi}^{-l} \end{bmatrix}^{\mathrm{H}}. \end{aligned} \tag{29}$$

The SVD of $\bar{\boldsymbol{Q}}_{\mathrm{E}}$ in which noncircular information contains is given by

$$\bar{\boldsymbol{Q}}_{\mathrm{E}} = \begin{bmatrix} \bar{\boldsymbol{U}}_s & \bar{\boldsymbol{U}}_n \end{bmatrix} \begin{bmatrix} \bar{\boldsymbol{\Sigma}}_{\mathrm{s}} & \boldsymbol{O} \\ \boldsymbol{O} & \boldsymbol{O} \end{bmatrix} \begin{bmatrix} \bar{\boldsymbol{V}}_s^{\mathrm{H}} \\ \bar{\boldsymbol{V}}_n^{\mathrm{H}} \end{bmatrix}. \tag{30}$$

Partitioning $\bar{\boldsymbol{U}}_n$ into two submatrices $\bar{\boldsymbol{U}}_{n1}$ and $\bar{\boldsymbol{U}}_{n2}$ with the same dimension, i.e.

$$\bar{\boldsymbol{U}}_n = \begin{bmatrix} \bar{\boldsymbol{U}}_{n1} \\ \bar{\boldsymbol{U}}_{n2} \end{bmatrix},$$

similar to NC-2q-MUSIC algorithm, we get the spatial spectrum function of NC-2q-MUSIC/ULA algorithm

$$\begin{aligned}\bar{f}(\theta) &= \bar{\boldsymbol{b}}_1^{\mathrm{H}}(\theta)\bar{\boldsymbol{U}}_{n1}\bar{\boldsymbol{U}}_{n1}^{\mathrm{H}}\bar{\boldsymbol{b}}_1(\theta) + \bar{\boldsymbol{b}}_2^{\mathrm{T}}(\theta)\bar{\boldsymbol{U}}_{n2}\bar{\boldsymbol{U}}_{n2}^{\mathrm{H}}\bar{\boldsymbol{b}}_2^*(\theta) \\ &\quad - 2\left\|\bar{\boldsymbol{b}}_1^{\mathrm{H}}(\theta)\bar{\boldsymbol{U}}_{n1}\bar{\boldsymbol{U}}_{n2}^{\mathrm{H}}\bar{\boldsymbol{b}}_2^*(\theta)\right\|. \end{aligned} \tag{31}$$

For $q = 2$, the computation of a $2q$th-order cumulant (i.e. fourth-order cumulant) is about $9L$ multiplications. Since $\bar{\boldsymbol{Q}}_{x1}$, $\bar{\boldsymbol{Q}}_{x2}$ and $\bar{\boldsymbol{Q}}_{x3}$ all are the $2M \times 2M$ matrix, about $108M^2L$ multiplications are needed to compute matrix $\bar{\boldsymbol{Q}}_{\mathrm{E}}$. In addition, the SVD of $\bar{\boldsymbol{Q}}_{\mathrm{E}}$ involves about $\mathrm{O}(64M^3)$ multiplications. Then the total computation of NC-4-MUSIC/ULA algorithm is about $108M^2L + \mathrm{O}(64M^3)$ multiplications. With the similar analysis, the total computation of NC-6-MUSIC/ULA algorithm is about $7200M^2L + \mathrm{O}(512M^3)$ multiplications. It follows that the gain of NC-2q-MUSIC/ULA algorithm compared to NC-2q-MUSIC algorithm is about $\mathrm{O}(M^3/8)$ and $\mathrm{O}(M^6/64)$ for $q = 2$ and 3, respectively, if the computation of $2q$th-order cumulant matrix dominates the total computation, i.e., $L \gg M^2$ and $L \gg M^3$ for $q = 2$ and 3, respectively. If the cost of SVD dominates the total computation, the gain is $8/M^3$ and $64/M^6$ for $q = 2$ and 3, respectively.

We extend the above results to an arbitrary even-order case. On the one hand, since the three matrices $\boldsymbol{Q}_{x1}$, $\boldsymbol{Q}_{x2}$ and $\boldsymbol{Q}_{x3}$ all are $M^q \times M^q$ and the matrices $\bar{\boldsymbol{Q}}_{x1}$, $\bar{\boldsymbol{Q}}_{x2}$ and $\bar{\boldsymbol{Q}}_{x3}$ all are $(2^{q-1}M) \times (2^{q-1}M)$, if the computation of $2q$th-order cumulant matrix dominates the total computation, the gain of NC-2q-MUSIC/ULA algorithm compared to NC-2q-MUSIC algorithm is about $(2^{q-1}M)^2/M^{2q} = (4/M^2)^{q-1}$. On the other hand, if the cost of SVD dominates the total computation, the gain is about $\mathrm{O}([2^qM/2M^q]^3) = \mathrm{O}((8/M^3)^{q-1})$ since $\boldsymbol{Q}_{\mathrm{E}}$ is $2M^q \times 2M^q$ matrix and $\bar{\boldsymbol{Q}}_{\mathrm{E}}$ is $(2^qM) \times (2^qM)$ matrix. Now we can draw the conclusion that the computation of NC-2q-MUSIC/ULA algorithm is much lower than that of NC-2q-MUSIC algorithm and the benefit grows with the increase of q.

5. Performance of NC-2q-MUSIC with modeling errors

In practical applications, when the number and locations of the sensors are given, the performance of the algorithm is mainly controlled by modeling errors such as array calibration errors or phase and amplitude residual mismatches between reception chains. For this reason, it is important to compute the asymptotic performance of NC-2q-MUSIC algorithm in the presence of modeling errors, showing off the influence of q and the noncircularity phase on the robustness of the algorithm.

5.1. Framework for modeling errors

In the presence of modeling errors, the steering vector becomes

$$\hat{\boldsymbol{a}}(\theta) = \boldsymbol{a}(\theta) + \tilde{\boldsymbol{a}}(\theta), \tag{32}$$

where $\hat{\boldsymbol{a}}(\theta)$ is the perturbed steering vector corrupted by modeling error vector $\tilde{\boldsymbol{a}}(\theta)$. The perturbed extended steering vector can be written as

$$\hat{\boldsymbol{b}}(\theta,\phi)=\boldsymbol{b}(\theta,\phi)+\tilde{\boldsymbol{b}}(\theta,\phi), \tag{33}$$

where

$$\tilde{\boldsymbol{b}}(\theta,\phi)=\begin{bmatrix}\boldsymbol{e}_1\\ \boldsymbol{e}_2\end{bmatrix}.$$

For $q=1$, $\boldsymbol{e}_1=\tilde{\boldsymbol{a}}(\theta)$, $\boldsymbol{e}_2=\tilde{\boldsymbol{a}}^*(\theta)\mathrm{e}^{-\mathrm{j}\phi}$, and for $q\geqslant 2$,

$$\begin{aligned}\boldsymbol{e}_1=&\sum_{u=0}^{l-1}\boldsymbol{a}(\theta)^{\otimes u}\otimes\tilde{\boldsymbol{a}}(\theta)\otimes\boldsymbol{a}(\theta)^{\otimes(l-u-1)}\otimes\boldsymbol{a}^*(\theta)^{\otimes(q-l)}\\&+\sum_{u=0}^{q-l-1}\boldsymbol{a}(\theta)^{\otimes l}\otimes\boldsymbol{a}^*(\theta)^{\otimes u}\otimes\tilde{\boldsymbol{a}}^*(\theta)\otimes\boldsymbol{a}^*(\theta)^{\otimes(q-l-u-1)},\end{aligned} \tag{34}$$

$$\boldsymbol{e}_2=\sum_{u=0}^{q-l}\boldsymbol{a}(\theta)^{*\otimes u}\otimes\tilde{\boldsymbol{a}}^*(\theta)\otimes\boldsymbol{a}^*(\theta)^{\otimes(q-u-1)}\,\mathrm{e}^{-\mathrm{j}\phi}. \tag{35}$$

To isolate the effects of these modeling errors on the DOA estimates, it will be assumed that the finite sample effects are negligible and that an exact measurement of the perturbed extended cumulant matrix $\hat{\boldsymbol{Q}}$ is available. For $q>1$

$$\hat{\boldsymbol{Q}}=(\boldsymbol{B}_{\mathrm{E}}+\tilde{\boldsymbol{B}}_{\mathrm{E}})\boldsymbol{\Gamma}(\boldsymbol{B}_{\mathrm{E}}+\tilde{\boldsymbol{B}}_{\mathrm{E}})^{\mathrm{H}}, \tag{36}$$

where $\tilde{\boldsymbol{B}}_{\mathrm{E}}=[\tilde{\boldsymbol{b}}(\theta_1,\phi_1),\tilde{\boldsymbol{b}}(\theta_2,\phi_2),\ldots,\tilde{\boldsymbol{b}}(\theta_D,\phi_D)]$ is the extended modeling error matrix and

$$\boldsymbol{B}_{\mathrm{E}}=\begin{bmatrix}\boldsymbol{B}_1\\ \boldsymbol{B}_2^*\boldsymbol{\Phi}^{-l}\end{bmatrix}=[\boldsymbol{b}(\theta_1,\phi_1),\boldsymbol{b}(\theta_2,\phi_2),\ldots,\boldsymbol{b}(\theta_D,\phi_D)].$$

To establish a link between the error terms of (36) and the noise subspace error matrix $\tilde{\boldsymbol{U}}_n$, we examine the noise eigenvectors of $\hat{\boldsymbol{Q}}_{\mathrm{E}}$ [12], defined by

$$\hat{\boldsymbol{U}}_n^{\mathrm{H}}\hat{\boldsymbol{Q}}_{\mathrm{E}}=\tilde{\boldsymbol{\Lambda}}\hat{\boldsymbol{V}}_n^{\mathrm{H}}\approx\tilde{\boldsymbol{\Lambda}}\boldsymbol{V}_n^{\mathrm{H}}, \tag{37}$$

where $\hat{\boldsymbol{U}}_n$ represents the perturbed noise eigenvectors and $\tilde{\boldsymbol{\Lambda}}$ represents the perturbed noise eigenvalues. Expending this equation using the model of (36) and eliminating the second-order error terms and terms involving $\boldsymbol{B}_{\mathrm{E}}^{\mathrm{H}}\boldsymbol{U}_n=\boldsymbol{O}$ leads to the following first-order approximation:

$$\tilde{\boldsymbol{U}}_n^{\mathrm{H}}\boldsymbol{B}_{\mathrm{E}}\boldsymbol{\Gamma}\boldsymbol{B}_{\mathrm{E}}^{\mathrm{H}}+\boldsymbol{U}_n\tilde{\boldsymbol{B}}_{\mathrm{E}}\boldsymbol{\Gamma}\boldsymbol{B}_{\mathrm{E}}^{\mathrm{H}}\approx\tilde{\boldsymbol{\Lambda}}\boldsymbol{V}_n^{\mathrm{H}}. \tag{38}$$

Multiplying (38) on the right by $\boldsymbol{B}_{\mathrm{E}}$ and eliminating terms involving $\boldsymbol{B}_{\mathrm{E}}^{\mathrm{H}}\boldsymbol{V}_n=\boldsymbol{O}$ then yields

$$\tilde{\boldsymbol{U}}_n^{\mathrm{H}}\boldsymbol{B}_{\mathrm{E}}\boldsymbol{\Gamma}\boldsymbol{B}_{\mathrm{E}}^{\mathrm{H}}\boldsymbol{B}_{\mathrm{E}}+\boldsymbol{U}_n\tilde{\boldsymbol{B}}_{\mathrm{E}}\boldsymbol{\Gamma}\boldsymbol{B}_{\mathrm{E}}^{\mathrm{H}}\boldsymbol{B}_{\mathrm{E}}\approx\boldsymbol{O}. \tag{39}$$

The matrix $\boldsymbol{\Gamma}\boldsymbol{B}_{\mathrm{E}}^{\mathrm{H}}\boldsymbol{B}_{\mathrm{E}}$ is full rank, thereby

$$\tilde{\boldsymbol{U}}_n^{\mathrm{H}}\boldsymbol{B}_{\mathrm{E}}\approx-\boldsymbol{U}_n^{\mathrm{H}}\tilde{\boldsymbol{B}}_{\mathrm{E}}. \tag{40}$$

For the case of $q=1$, the same relationship can be derived following the steps of (37)–(40).

5.2. First-order error analysis

With modeling errors, (20) becomes

$$\hat{f}(\theta,\phi)=\boldsymbol{b}^{\mathrm{H}}(\theta,\phi)\hat{\boldsymbol{U}}_n\hat{\boldsymbol{U}}_n^{\mathrm{H}}\boldsymbol{b}(\theta,\phi). \tag{41}$$

Assuming $(\hat{\theta}_i,\hat{\phi}_i)$ is the estimated directions of source $i(1\leqslant i\leqslant D)$ where its real directions is (θ_i,ϕ_i), for small enough modeling errors, we define some denotations as follows:

$$\begin{aligned}\hat{f}'_{\theta}(i)&\triangleq\left.\frac{\partial\hat{f}(\theta,\phi)}{\partial\theta}\right|_{(\theta,\phi)=(\hat{\theta}_i,\hat{\phi}_i)}\\&=2\mathrm{Re}\left\{\boldsymbol{b}'^{\mathrm{H}}_{\theta}(i)\,\hat{\boldsymbol{U}}_n\hat{\boldsymbol{U}}_n^{\mathrm{H}}\boldsymbol{b}(\theta_i,\phi_i)\right\}\\&\approx2\mathrm{Re}\left\{\boldsymbol{b}'^{\mathrm{H}}_{\theta}(i)\,\boldsymbol{U}_n\tilde{\boldsymbol{U}}_n^{\mathrm{H}}\boldsymbol{b}(\theta_i,\phi_i)\right\}\\&\approx-2\mathrm{Re}\left\{\boldsymbol{b}'^{\mathrm{H}}_{\theta}(i)\,\boldsymbol{U}_n\boldsymbol{U}_n^{\mathrm{H}}\tilde{\boldsymbol{b}}(\theta_i,\phi_i)\right\},\end{aligned} \tag{42}$$

$$\begin{aligned}\hat{f}'_{\phi}(i)&\triangleq\left.\frac{\partial\hat{f}(\theta,\phi)}{\partial\phi}\right|_{(\theta_i,\phi_i)=(\hat{\theta}_i,\hat{\phi}_i)}\\&=2\mathrm{Re}\left\{\boldsymbol{b}'^{\mathrm{H}}_{\phi}(i)\hat{\boldsymbol{U}}_n\hat{\boldsymbol{U}}_n^{\mathrm{H}}\boldsymbol{b}(\theta_i,\phi_i)\right\}\\&\approx2\mathrm{Re}\left\{\boldsymbol{b}'^{\mathrm{H}}_{\phi}(i)\boldsymbol{U}_n\tilde{\boldsymbol{U}}_n^{\mathrm{H}}\boldsymbol{b}(\theta_i,\phi_i)\right\}\\&\approx-2\mathrm{Re}\left\{\boldsymbol{b}'^{\mathrm{H}}_{\phi}(i)\boldsymbol{U}_n\boldsymbol{U}_n^{\mathrm{H}}\tilde{\boldsymbol{b}}(\theta_i,\phi_i)\right\},\end{aligned} \tag{43}$$

$$\begin{aligned}f''_{\theta,\theta}(i)&\triangleq\left.\frac{\partial^2 f(\theta,\phi)}{\partial^2\phi}\right|_{(\theta_i,\phi_i)=(\hat{\theta}_i,\hat{\phi}_i)}\\&=2\boldsymbol{b}'^{\mathrm{H}}_{\theta}(i)\boldsymbol{U}_n\boldsymbol{U}_n^{\mathrm{H}}\boldsymbol{b}'_{\theta}(i),\end{aligned} \tag{44}$$

$$\begin{aligned}f''_{\phi,\phi}(i)&\triangleq\left.\frac{\partial^2 f(\theta,\phi)}{\partial^2\phi}\right|_{(\theta_i,\phi_i)=(\hat{\theta}_i,\hat{\phi}_i)}\\&=2\boldsymbol{b}'^{\mathrm{H}}_{\phi}(i)\boldsymbol{U}_n\boldsymbol{U}_n^{\mathrm{H}}\boldsymbol{b}'_{\phi}(i),\end{aligned} \tag{45}$$

$$\begin{aligned}f''_{\theta,\phi}(i)&\triangleq\left.\frac{\partial^2 f(\theta,\phi)}{\partial\theta\,\partial\phi}\right|_{(\theta_i,\phi_i)=(\hat{\theta}_i,\hat{\phi}_i)}\\&=2\left\{\boldsymbol{b}'^{\mathrm{H}}_{\theta}(i)\boldsymbol{U}_n\boldsymbol{U}_n^{\mathrm{H}}\boldsymbol{b}'_{\phi}(i)\right\}\\&=f''_{\phi,\theta}\triangleq\left.\frac{\partial^2 f(\theta,\phi)}{\partial\phi\,\partial\theta}\right|_{(\theta_i,\phi_i)=(\hat{\theta}_i,\hat{\phi}_i)},\end{aligned} \tag{46}$$

where

$$\boldsymbol{b}'_\theta(i) \triangleq \left.\frac{\partial \boldsymbol{b}(\theta,\phi)}{\partial\theta}\right|_{(\theta,\phi)=(\hat{\theta}_i,\hat{\phi}_i)}, \quad \boldsymbol{b}'_\phi(i) \triangleq \left.\frac{\partial \boldsymbol{b}(\theta,\phi)}{\partial\phi}\right|_{(\theta,\phi)=(\hat{\theta}_i,\hat{\phi}_i)}.$$

In (42) and (43), the second-order error terms and terms involving $\boldsymbol{B}_{\mathrm{E}}^{\mathrm{H}}\boldsymbol{U}_n = \boldsymbol{O}$ are neglected.

Since $(\hat{\theta}_i, \hat{\phi}_i)$ is the estimated directions of source i $(1 \leqslant i \leqslant D)$ $(\hat{\theta}_i, \hat{\phi}_i)$ satisfies

$$\left.\frac{\partial \hat{f}(\theta,\phi)}{\partial\theta}\right|_{(\theta,\phi)=(\hat{\theta}_i,\hat{\phi}_i)} = 0 \tag{47}$$

and

$$\left.\frac{\partial \hat{f}(\theta,\phi)}{\partial\phi}\right|_{(\theta,\phi)=(\hat{\theta}_i,\hat{\phi}_i)} = 0. \tag{48}$$

We straightforwardly obtain the following first-order perturbation expansion [7,12,13]:

$$\begin{aligned}
&\hat{f}'_\theta(i) + (\hat{\theta}_i - \theta_i) f''_{\theta,\theta}(i) + (\hat{\phi}_i - \phi_i) f''_{\theta,\phi}(i) = 0,\\
&\hat{f}'_\phi(i) + (\hat{\theta}_i - \theta_i) f''_{\theta,\phi}(i) + (\hat{\phi}_i - \phi_i) f''_{\phi,\phi}(i) = 0.
\end{aligned} \tag{49}$$

It is easy to derive from the above equation

$$\hat{\theta}_i - \theta_i = \frac{\hat{f}'_\phi(i) f''_{\theta,\phi}(i) - \hat{f}'_\theta(i) f''_{\phi,\phi}(i)}{f''_{\theta,\theta}(i) f''_{\phi,\phi}(i) - [f''_{\theta,\phi}(i)]^2}. \tag{50}$$

For the case where $\tilde{\boldsymbol{b}}(\theta_i, \phi_i)$ is zero-mean realization of some known perturbation model, it is clear that $E\{\hat{\theta}_i - \theta\} \approx 0$ and the variance of the estimation error is shown that

$$\begin{aligned}
E\{(\hat{\theta}_i - \theta_i)^2\} = \frac{1}{\gamma^2}\Big[&[f''_{\phi,\phi}(i)]^2 E\left\{[\hat{f}'_\theta(i)]^2\right\}\\
&+ [f''_{\theta,\phi}(i)]^2 E\left\{[\hat{f}'_\phi(i)]^2\right\}\\
&-2 f''_{\theta,\phi}(i) f''_{\phi,\phi}(i) E\left\{\hat{f}'_\theta(i)\hat{f}'_\phi(i)\right\}\Big]
\end{aligned} \tag{51}$$

with

$$\gamma \triangleq f''_{\theta,\theta}(i) f''_{\phi,\phi}(i) - [f''_{\theta,\phi}(i)]^2.$$

Note that for two scalar-valued complex variables, u and v, we have $\mathrm{Re}\{u\}\mathrm{Re}\{v\} = \frac{1}{2}[\mathrm{Re}\{uv\} + \mathrm{Re}\{uv^*\}]$ [13]. Then the three expectations in (51) can be expressed as

$$\begin{aligned}
E\left\{[\hat{f}'_\theta(i)]^2\right\} = 2\mathrm{Re}\Big\{&\boldsymbol{b}'^{\mathrm{H}}_\theta(i)\boldsymbol{\Pi}\boldsymbol{C}_{b,1}\boldsymbol{\Pi}\boldsymbol{b}'_\theta(i)\\
&+\boldsymbol{b}'^{\mathrm{H}}_\theta(i)\boldsymbol{\Pi}\boldsymbol{C}_{b,2}\boldsymbol{\Pi}^{\mathrm{T}}\boldsymbol{b}'^{*}_\theta(i)\Big\},
\end{aligned} \tag{52}$$

$$\begin{aligned}
E\left\{[\hat{f}'_\phi(i)]^2\right\} = 2\mathrm{Re}\Big\{&\boldsymbol{b}'^{\mathrm{H}}_\phi(i)\boldsymbol{\Pi}\boldsymbol{C}_{b,1}\boldsymbol{\Pi}\boldsymbol{b}'_\phi(i)\\
&+\boldsymbol{b}'^{\mathrm{H}}_\phi(i)\boldsymbol{\Pi}\boldsymbol{C}_{b,2}\boldsymbol{\Pi}^{\mathrm{T}}\boldsymbol{b}'^{*}_\phi(i)\Big\},
\end{aligned} \tag{53}$$

$$\begin{aligned}
E\left\{\hat{f}'_\theta(i)\hat{f}'_\phi(i)\right\} = 2\mathrm{Re}\Big\{&\boldsymbol{b}'^{\mathrm{H}}_\theta(i)\boldsymbol{\Pi}\boldsymbol{C}_{b,1}\boldsymbol{\Pi}\boldsymbol{b}'_\phi(i)\\
&+\boldsymbol{b}'^{\mathrm{H}}_\theta(i)\boldsymbol{\Pi}\boldsymbol{C}_{b,2}\boldsymbol{\Pi}^{\mathrm{T}}\boldsymbol{b}'^{*}_\phi(i)\Big\},
\end{aligned} \tag{54}$$

with

$$\boldsymbol{\Pi} \triangleq \boldsymbol{U}_n\boldsymbol{U}_n^{\mathrm{H}} = \boldsymbol{I}_{2M^q} - \boldsymbol{B}_{\mathrm{E}}(\boldsymbol{B}_{\mathrm{E}}^{\mathrm{H}}\boldsymbol{B}_{\mathrm{E}})^{-1}\boldsymbol{B}_{\mathrm{E}}^{\mathrm{H}},$$

$$\boldsymbol{C}_{b,1} = E\{\tilde{\boldsymbol{b}}(\theta_i,\phi_i)\tilde{\boldsymbol{b}}^{\mathrm{H}}(\theta_i,\phi_i)\}$$

and

$$\boldsymbol{C}_{b,2} = E\{\tilde{\boldsymbol{b}}(\theta_i,\phi_i)\tilde{\boldsymbol{b}}^{\mathrm{T}}(\theta_i,\phi_i)\}.$$

Correspondingly, for $2q$-MUSIC algorithm with modeling errors, we have

$$\begin{aligned}
&E\left\{(\hat{\theta}_i - \theta_i)^2\right\}\\
&= \frac{2}{[f''_\theta(\theta_i)]^2}\mathrm{Re}\Big\{\boldsymbol{b}'^{\mathrm{H}}_1(\theta_i)\boldsymbol{\Pi}_1 E\{\boldsymbol{e}_1(\theta_i)\boldsymbol{e}_1^{\mathrm{H}}(\theta_i)\}\\
&\quad\times\boldsymbol{\Pi}_1\boldsymbol{b}'_1(\theta_i) + \boldsymbol{b}'^{\mathrm{H}}_1(\theta_i)\boldsymbol{\Pi}_1 E\{\boldsymbol{e}_1(\theta_i)\boldsymbol{e}_1^{\mathrm{T}}(\theta_i)\}\boldsymbol{\Pi}_1^{\mathrm{T}}\boldsymbol{b}'^{*}_1(\theta_i)\Big\}
\end{aligned} \tag{55}$$

with

$$\boldsymbol{\Pi}_1 \triangleq \boldsymbol{I}_{M^q} - \boldsymbol{B}_1(\boldsymbol{B}_1^{\mathrm{H}}\boldsymbol{B}_1)^{-1}\boldsymbol{B}_1^{\mathrm{H}},$$

$$f''_\theta(\theta_i) \triangleq 2\boldsymbol{b}'^{H}_1(\theta_i)\boldsymbol{\Pi}_1\boldsymbol{b}'_1(\theta_i),$$

$$\boldsymbol{b}'_1(\theta_i) \triangleq \left.\frac{\mathrm{d}\boldsymbol{b}_1(\theta)}{\mathrm{d}\theta}\right|_{(\theta=\theta_i)}.$$

It is shown in (51), the robustness of the NC-$2q$-MUSIC algorithm depends on q and the noncircularity phases of the signals. This point will be further demonstrated by the illustrations in the next subsection.

5.3. Illustrations

To illustrate the previous results, we assume that two statistically independent sources from the directions [87.3°,92.7°] are received by a ULA of $M = 3$ omnidirectional sensors with half a wavelength apart. The modeling error vectors $\tilde{\boldsymbol{a}}(\theta_i)$ $(1 \leqslant i \leqslant 2)$ are assumed to be zero-mean statistically independent circular Gaussian vectors such that $E\{\tilde{\boldsymbol{a}}(\theta_i)\tilde{\boldsymbol{a}}^{\mathrm{H}}(\theta_j)\} = \sigma^2\delta_{ij}\boldsymbol{I}_M$ and $E\{\tilde{\boldsymbol{a}}(\theta_i)\tilde{\boldsymbol{a}}^{\mathrm{T}}(\theta_j)\} = \boldsymbol{O}$, where $\sigma = 0.01745$ which corresponds, for example, to a phase error with a standard deviation of 1° with no amplitude error. Under these assumptions, Fig. 1

shows, for $q = 1$, 2, 3 and $l = 1$, the root mean square error (RMSE) of the source 1 (it is similar for source 2) and the ratios of RMSEs between NC-2q-MUSIC and 2q-MUSIC algorithms as a function of the noncircularity phase separation (by virtue of numerical examples, the different theoretical RMSE depends on θ_1, θ_2, ϕ_1, ϕ_2 by only $\pi\cos\theta_1-\pi\cos\theta_2$ and $\phi_1-\phi_2$). The RMSE is defined by $\sqrt{E\{(\hat{\theta}-\theta)^2\}}$.

Fig. 1 shows, for each value of noncircularity phase separation, a decreasing RMSE as q increases. Besides, for the same q, the RMSE of NC-2q-MUSIC algorithm is no more than that of 2q-MUSIC algorithm. To our interest, the RMSE of NC-2q-MUSIC algorithm is particularly high for some area of noncircularity phase separation (around 34° for this scenario, and by virtue of numerical simulations, it may be different when the DOA separation varies), and the RMSE of NC-2q-MUSIC algorithm in this point equals that of 2q-MUSIC algorithm and decreases rapidly as q increases. We name this point the critical point and the area around this point the critical area. For two noncircular signals scenario, the robustness of the NC-2q-MUSIC algorithm is the same as 2q-MUSIC algorithm when the noncircularity phase separation is close to critical area, while the noncircularity phase separation is at random and few in this area in practice. Consequently, in the presence of modeling errors, the NC-2q-MUSIC algorithm is more robust than the 2q-MUSIC algorithm from statistical points.

It is also shown in Fig. 1(a) that, when the noncircularity phase separation is far from the critical area, the robustness to modeling errors of the NC-2q-MUSIC algorithms for different q is almost the same and the NC-2-MUSIC algorithm is preferred. When the noncircularity phase separation is near or within the critical area, in view of robustness, the 2q-MUSIC algorithm is preferred rather than the NC-2q-MUSIC algorithm because of their similar robustness to modeling errors, and 4-MUSIC is preferred according to its robustness to modeling errors and moderate computational complexity.

It should be reminded that the illustrations presented in this section are computed for exact statistics of the data. Simulation results in the case of large number of snapshots and of large SNR can validate the accordance between the theoretical and empirical results. Estimated statistics will be considered in the next section.

6. Simulation results

We now evaluate the DOA estimation performance of NC-2q-MUSIC algorithm for a few cases by computer simulations. Specifically, the estimation capacity, estimation precision and robustness to modeling errors are studied. We assume that statistically independent BPSK signals are received by a ULA of $M = 3$ omnidirectional sensors spaced half a wavelength apart. The BPSK signals have the same symbol duration and the same input SNR. The noise is complex circular Gaussian.

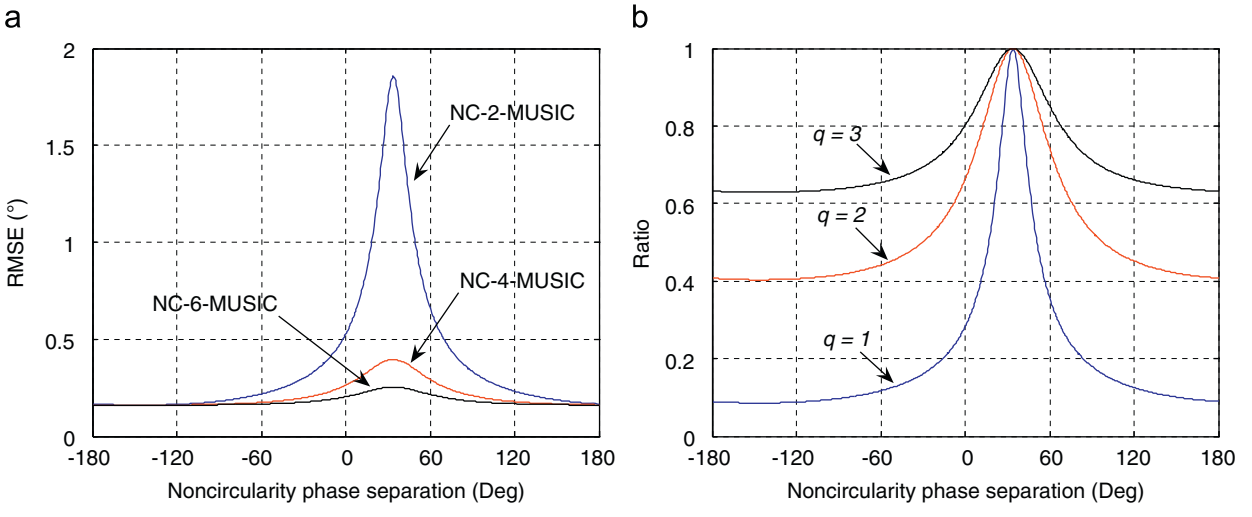

Fig. 1. Performance of NC-2q-MUSIC algorithm with modeling errors: (a) RMSEs of NC-2q-MUSIC algorithms and (b) the ratios of RMSEs between the two kinds of algorithms.

6.1. Case 1 (estimation capacity)

$2q$-MUSIC algorithm with $q \geqslant 2$ can handle more signals than sensors due to its capability of aperture extension [4]. For NC-$2q$-MUSIC, the steering matrix is extended further, so that the aperture is further extended. Therefore, NC-$2q$-MUSIC algorithm can handle more signals than $2q$-MUSIC algorithm. For ULA, the number for NC-$2q$-MUSIC is $(q+l)(M-1)$ according to the virtual array concept depicted in [4,10] while the number for $2q$-MUSIC algorithm is only $q(M-1)$ [4]. Suppose six independent BPSK signals impinge on the array, the phases of the signals are all zeros, the number of snapshots is 2000, the SNR is 20 dB and the DOAs are [40°,60°,80°,100°,120°,140°], respectively, Fig. 2(a) indicates results from 10 realizations of NC-4-MUSIC algorithm (here, $l = 1$). Supposing that eight BPSK signals impinge on the array from directions [35°,55°,70°,85°,100°,115°,130°, 150°] and the number of snapshots is 5000, Fig. 2(b) shows results from 10 realizations of NC-6-MUSIC algorithm (here, $l = 1$, corresponding to the above scenario for NC-4-MUSIC). The number of noncircular signals that NC-4-MUSIC and NC-6-MUSIC algorithms can handle are 6 and 8, respectively, while the number for 4-MUSIC and 6-MUSIC are 4 and 6, respectively. It is evident that the estimation capacity of NC-$2q$-MUSIC algorithm is larger than that of $2q$-MUSIC algorithm.

6.2. Case 2 (estimation precision)

The RMSE of $2q$-MUSIC algorithm in the case of $q \geqslant 2$ is better than MUSIC (i.e., 2-MUSIC) because the $2q$-MUSIC algorithm extends the aperture of the array and narrows the 3-dB beam width of the array [4]. The NC-$2q$-MUSIC algorithm has lower RMSE than $2q$-MUSIC due to its further aperture extension capability. We will demonstrate this point in this subsection with computer simulations. Considering two statistically independent BPSK signals impinging on the array from the directions [87.3°,92.7°], assuming the phases of the two signals distribute uniformly in the range of $[0,2\pi]$ and the number of snapshots is 2000, Fig. 3(a) shows behaviors of the two kinds of algorithms when the signal-to-noise ratio (SNR) varied from 0 to 15 dB. Fig. 3(b) shows how the number of snapshots affects the RMSE performance of the algorithms, where the two signals have the same SNR equal to 5 dB. Fig. 3(c) illustrates how the angular separation affects the performance of the algorithms, where the two signals impinge on the array symmetrically around 90° with the same SNR equal to 5 dB and the same number of snapshots equal to 2000. The RMSEs are estimated from 300 realizations and the RMSE of the ith ($i = 1, 2$) DOA is defined by $\sqrt{\sum_{j=1}^{300}[\hat{\theta}_i(j) - \theta_i(j)]^2/300}$, which is an estimate of the RMSE introduced in Section 5.3, where $\hat{\theta}_i$ is the

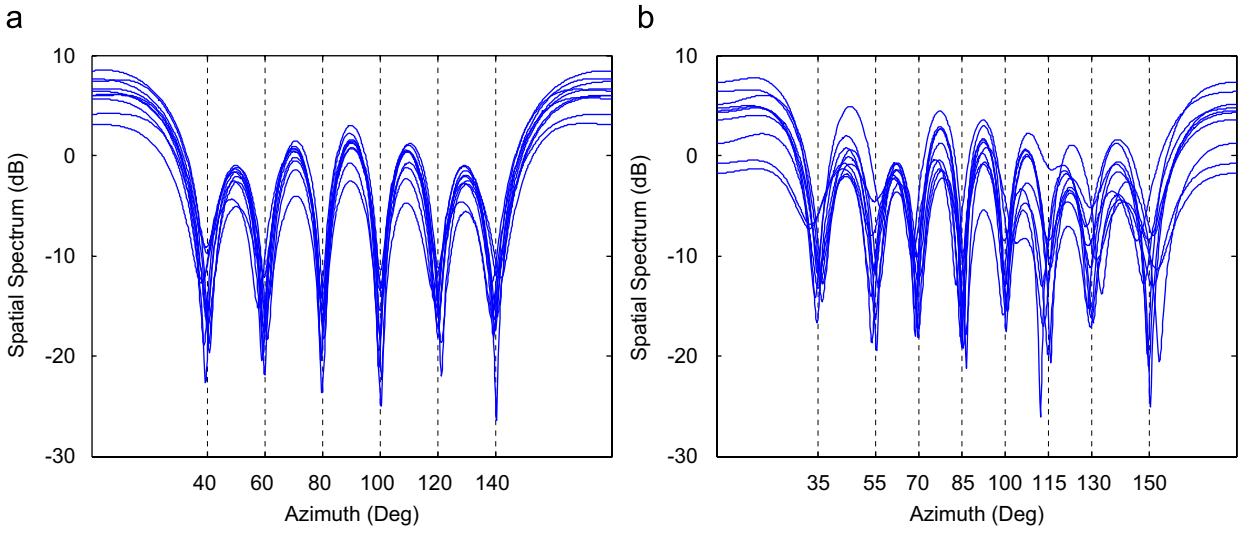

Fig. 2. Estimation capacity of NC-$2q$-MUSIC algorithm: (a) NC-4-MUSIC and (b) NC-6-MUSIC.

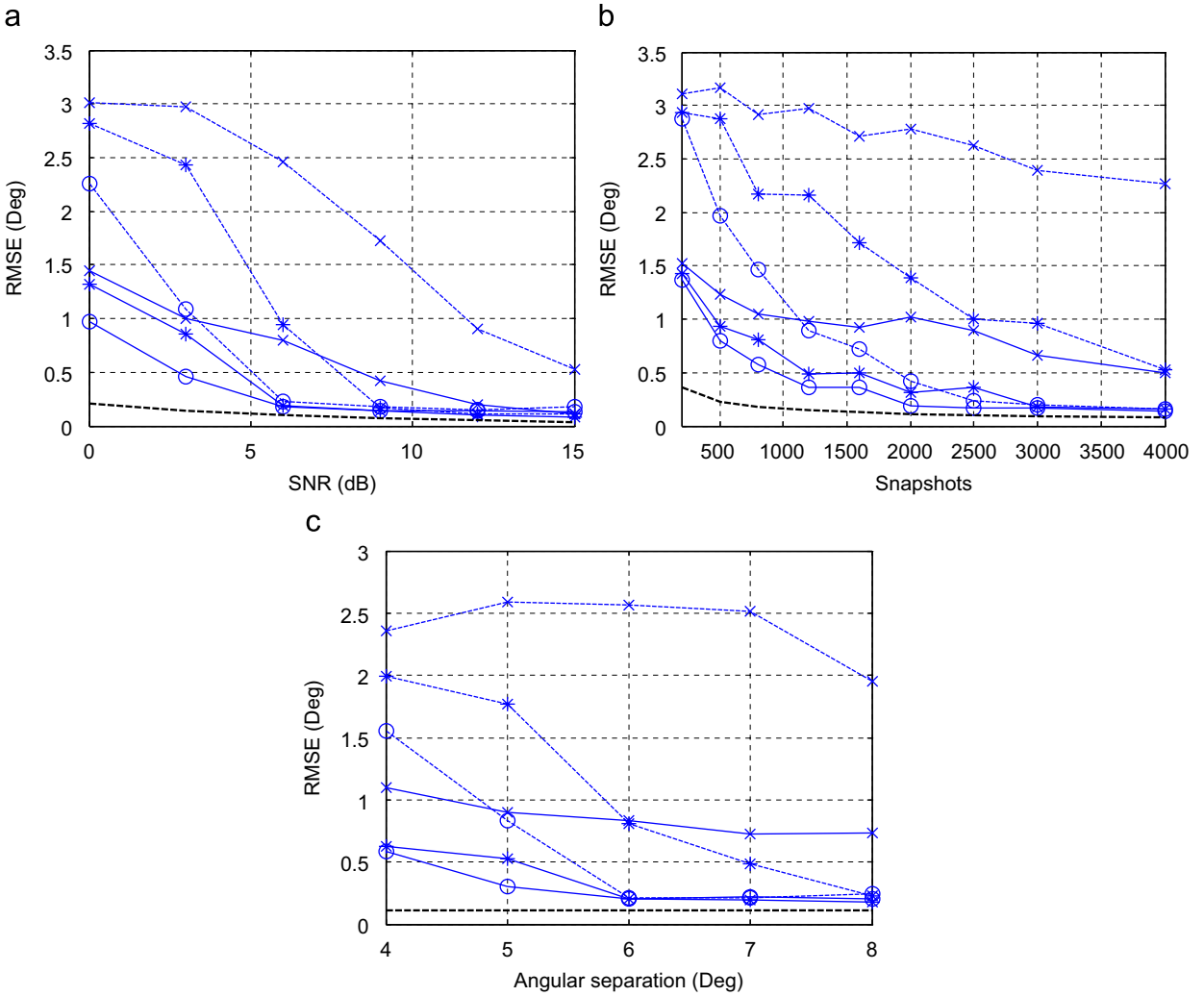

Fig. 3. Estimation precision of the two kinds of algorithms without modeling errors: (a) RMSE vs. SNR, (b) RMSE vs. snapshots and (c) RMSE vs. angular separation.

estimated value of θ_i. Especially, if there is only one minimum in the spatial spectrum, we define both estimated angles as the angle corresponding to the only minimum. In the simulations, $l = 1$ when $q \geqslant 2$, and the marker "$\times$"denotes second-order algorithms, "*"for fourth-order, "o" for sixth-order, the solid line denotes NC-2q-MUSIC, the dashed line denotes 2q-MUSIC and the thick dashed line denotes the Cramer–Rao bound (CRB) [14] for BPSK signals. It is obvious from Fig. 3 that the estimation precision of NC-2q-MUSIC algorithm are better than 2q-MUSIC of the same order, and NC-2q-MUSIC has increasing estimation precision as q increases. When SNR, the number of snapshots and the angular separation are relatively large, the RMSEs are close to the corresponding CRBs.

6.3. Case 3 (robustness to modeling errors)

In this case, the modeling errors are assumed to be zero-mean statistically independent circular Gaussian variables with $\sigma = 0.01745$ which corresponds, for example, to a phase error with a standard deviation of 1° with no amplitude error. Other simulation conditions are the same as in case 2. The RMSEs of the two kinds of algorithms versus SNR, the number of snapshots and the angular separation are given in Fig. 4. It shows off the best behavior of NC-6-MUSIC with respect to NC-2-MUSIC and NC-4-MUSIC and the better behavior of NC-2q-MUSIC with respect to 2q-MUSIC. Similar to the behavior of 2q-MUSIC which is less insensitive to modeling errors with the increase of q

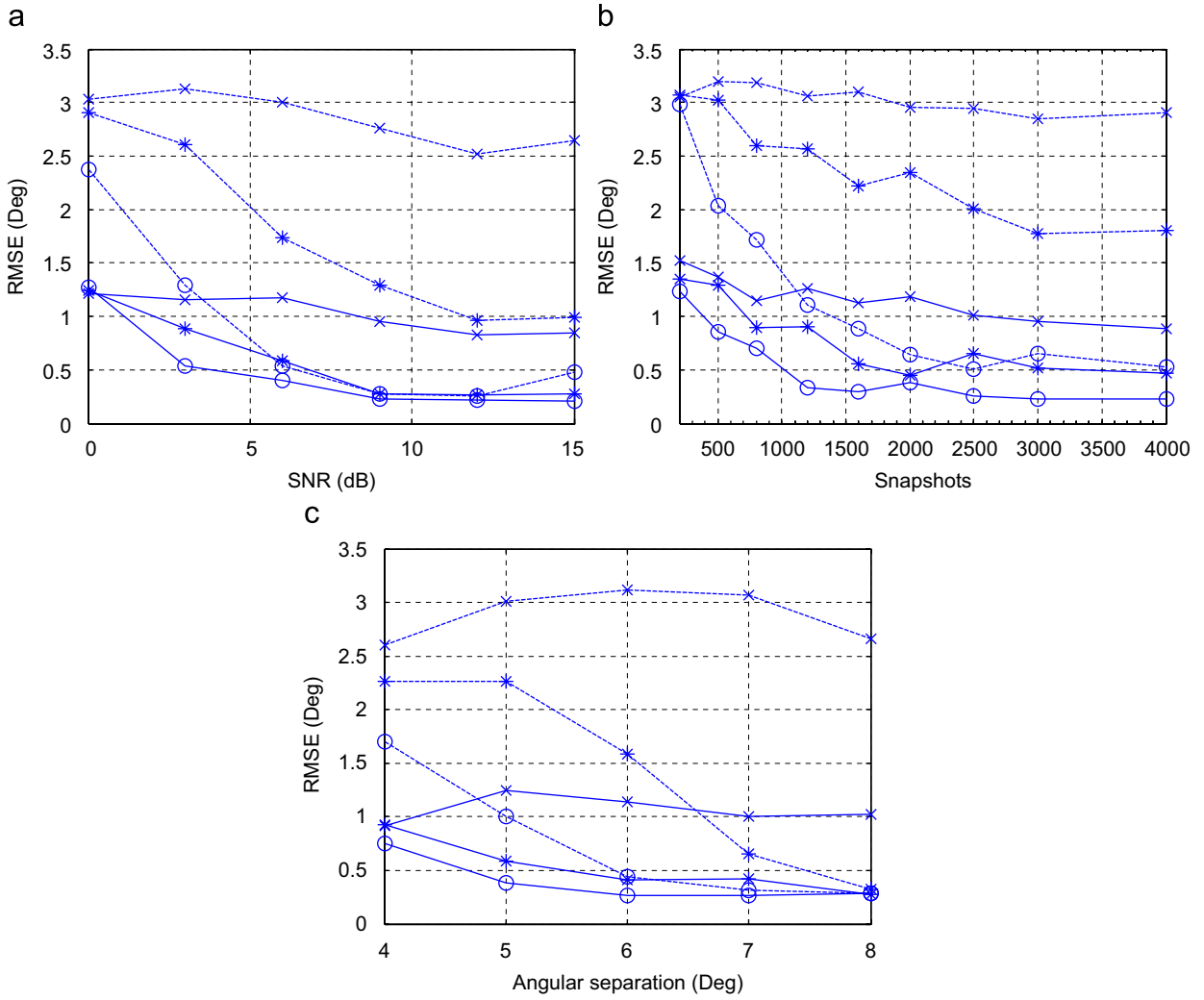

Fig. 4. Estimation precision of the two kinds of algorithms with modeling errors: (a) RMSE vs. SNR, (b) RMSE vs. snapshots and (c) RMSE vs. angular separation.

[4], NC-2q-MUSIC algorithm has the increasing robustness as q increases (in contrast to Fig. 3), which is consistent with the analysis in Section 5.

7. Conclusions

In this paper, an extension of the 2q-MUSIC algorithm to noncircular applications has been introduced, giving rise to the so-called NC-2q-MUSIC algorithms. The computational complexity of NC-2q-MUSIC and its uniform linear array (ULA) version is analyzed. The latter alleviates the computational load for $q \geqslant 2$. The estimation precision of NC-2q-MUSIC is better than 2q-MUSIC of the same order, and NC-2q-MUSIC has the increasing robustness to modeling errors as q increases. Simulation results validate all the conclusions about NC-2q-MUSIC algorithms.

Acknowledgement

The authors acknowledge support from National Natural Science Foundation of China (No. 60502040) and would like to thank the anonymous reviewers for their useful comments and suggestions that significantly improved the paper.

References

[1] R.O. Schmidt, Multiple emitter location and signal parameter estimation, IEEE Trans. Antennas Propag. 34 (1986) 276–280.

[2] B. Porat, B. Friedlander, Direction finding algorithms based on high-order statistics, IEEE Trans. Signal Process. 39 (1991) 2016–2023.
[3] M.C. Dogan, J.M. Mendel, Application of cumulants to array processing—part I: aperture extension and array calibration, IEEE Trans. Signal Process. 43 (1995) 1200–1216.
[4] P. Chevalier, A. Ferreol, L. Albera, High resolution direction finding from higher order statistics: the 2q-MUSIC algorithm, IEEE Trans. Signal Process. 54 (2006) 2986–2997.
[5] P. Charge, Y. Wang, J. Saillard, A noncircular sources direction finding method using polynomial rooting, Signal Processing 81 (2001) 1765–1770.
[6] M. Haardt, F. Romer, Enhancements of unitary ESPRIT for non-circular sources, in: Proceedings of the ICASSP, 2004, pp. 101–104.
[7] H. Abeida, J.P. Delmas, MUSIC-like estimation of direction of arrival for noncircular sources, IEEE Trans. Signal Process. 54 (2006) 2678–2690.
[8] J.P. Delmas, H. Abeida, Stochastic Cramer–Rao bound for noncircular signals with applications to DOA estimation, IEEE Trans. Signal Process. 52 (2004) 3192–3199.
[9] H. Abeida, J.P. Delmas, Gaussian Cramer–Rao bound for direction estimation of noncircular signals in unknown noise fields, IEEE Trans. Signal Process. 53 (2005) 4610–4618.
[10] P. Chevalier, L. Albera, F.A. Ferreol, P. Comon, On the virtual array concept for higher order array processing, IEEE Trans. Signal Process. 53 (2005) 1254–1271.
[11] T. Kaiser, J.M. Mendel, Covariance of finite-sample cumulants in array-processing, in: 1997 Proceedings of the IEEE Signal Processing Workshop on High-Order Statistics, pp. 306–310.
[12] A.L. Swindlehurst, T. Kailath, A performance analysis of subspace-based methods in the presence of model errors, part I: the MUSIC algorithm, IEEE Trans. Signal Process. 40 (1992) 1758–1774.
[13] P. Stoica, A. Nehorai, MUSIC, maximum likelihood, and Cramer–Rao bound, IEEE Trans. Acoust. Speech Signal Process. 37 (1989) 720–741.
[14] J.P. Delmas, H. Abeida, Cramer–Rao bound of DOA estimates for BPSK and QPSK modulated signals, IEEE Trans. Signal Process. 54 (2006) 117–126.